Microstructural study of an aluminium sheet deformed by multistage process

Gyula Pál[a,b]*, Purnima Chakravarty[a,b], János György Bátorfi[a,b], Jurij Sidor[a]

[a] *ELTE, Faculty of Informatics, Savaria Institute of Technology*
[b] *ELTE, Faculty of Science, Doctoral School of Physics*

ABSTRACT

The current as well as the future industrial market for Aluminium (Al) is huge and various research is being under work regarding the usability of Aluminium. However, during the deep drawing of Aluminium several issues can be developed and some of them are originated from the fundamental material properties. One of these factors is the material texture, which is the preferred orientation of the constituent polycrystalline Al, and the characteristic texture is affected by different rolling and annealing recipes. To investigate the material texture, symmetric and asymmetric rolling trials were performed on a commercially available Al 1050 sample. Energy-dispersive X-ray Spectroscopy (EDX), and Electron Backscatter Diffraction (EBSD) scanning has performed to determine the material composition and the crystallographic orientations of the investigated samples.

Keywords: *aluminium, microstructure, texture*

1. Introduction

Aluminium as a material is widely used in the industry because of its low density and high corrosion resistance. There are several methods already existing in the industry for the processing of Aluminium that can provide optimum material properties. The hollow geometry parts i.e. cups are generally manufactured with relatively small wall thickness, which is commonly produced by the method of deep drawing. However, during the process of deep drawing 5 main issues can be emerged, namely frame wrinkling, wall wrinkling, tearing, earing, and surface scratches [1]. These manufacturing defects originate from different sources. Many manufacturing defects can arise from the non-conformance of manufacturing conditions such as worn out or poorly maintained production equipment, or ignoring of work instructions. Some defects i.e. earing and tearing are caused by the ignorance of different mechanical properties of Aluminium e.g. yield strength and planar anisotropy compared to the better deep-drawability characteristics of steel [2].

The advancement in Aluminium research suggests that it is possible to develop materials with better mechanical properties by non-chemical processes [3]. This is the motivation of the current study. Generally, it is possible to influence the following properties of a base material by [4]:

- The chemical composition;
- Different heat treatment methods;
- Mechanical processing.

© ELTE, Faculty of Informatics, Savaria Institute of Technology, 2022
*Corresponding author: Gyula Pál, pg@inf.elte.hu
https://doi.org/10.37775/EIS.2022.2.6

The production steps of sheets classically consist of the hot and cold rolling of casted ingots with optional intermediate and final annealing. During conventional i.e. symmetric rolling, the material passes between two rolls, which rotates opposite to each other with the same angular velocity [5]. However, in the last few decades, experiments are conducted using asymmetric rolling, i.e. the rolls are rotating with a different angular velocity, bringing in an extra shear strain into the material. These processing steps have a significant effect on the mechanical properties, which can be explained at the microstructural level [6].

The atoms of the metals - like Aluminium – forms microscopic crystal lattice. These crystals form groups, where they are grow in the same direction, creating the grains of a polycrystalline microstructure [7]. The dimension and shape of the polycrystal can be evaluated by several methods like the electron microscope, X-Ray diffraction, and Synchrotron Radiation [8]. Nowadays one of the most common methods to characterise polycrystalline material is scanning electron microscope equipped with an electron backscatter diffraction detector (EBSD) [9]. When the electron beam is projected on a specimen under consideration, the instrument detects the backscattered electrons, resulting in the formation of Kikuchi-patterns via the phenomenon of diffraction [10]. These patterns can reveal the orientation of crystals in the examined area. The repetition of this test on every point of a selected sample area shows a grain orientation map called inverse pole figure (IPF). The IPF can reveal the shapes, dimensions, and orientations of the grains spotted on the specimen area, providing necessary information for the analysis of microstructure [11].

Very important characteristic of a material is the texture, which is the orientation distribution of its crystals [12]. To characterize the texture of materials, quite often the orientation distribution function (ODF) is employed, which shows all of the crystallographic orientations in Euler space [11], based on their angle deviations compared to a specified direction, i.e. rolling direction.

The common directions i.e. textures have received unique names, also specified texture groups are existing which are called fibers, because these typical groups are creating elongated fiber-like patterns within the Euler space [13]. The most common fibers are the β-fiber created by the Copper, S, and Brass textures, the α-fiber ($\langle 110 \rangle // \mathrm{ND}$) and the γ-fiber ($\langle 111 \rangle // \mathrm{ND}$). In the Face Centered Cubic (FCC) metals, the α-fiber and β-fiber components are indicative of plane strain compression, while the γ-fiber tends to appear after shear [14–16]. However, annealing can transform the deformation textures to recrystallization textures, like the Cube ($100\ \langle 001 \rangle$) [11, 17].

Several studies were published about the connection of microstructure, texture, and material characteristics [18–24]. Based on this literature sources, it is possible to develop recipe e.g. rolling and annealing methods, which help to achieve the desired mechanical properties i.e. the normal anisotropy (Lankford number) over 1.1, and planar anisotropy correlating to 0 [25]. The most preferable textures to achieve these values are the random and shear textures [3].

The change of mechanical properties, i.e. the hardness is connected to the accumulation of deformation, and the evolution of dislocation density. These crystal defects are responsible for the work hardenings, thus measuring the hardness we can estimate the dislocation density and the driving force for recrystallization [26].

In this study, we are analysing the rolling experiment, which contains one step of asymmetric rolling and two steps of symmetric rolling followed by a particular annealing routine. The evolution of microstructure, texture, and mechanical properties during the conducted thermo-mechanical processing (TMP) steps has been reported in this work.

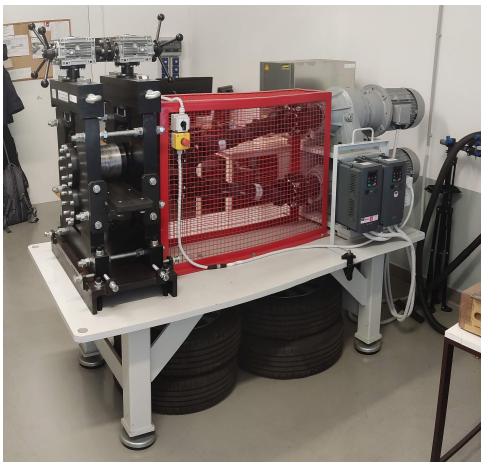

Figure 1. Laboratory rolling mill

2. Methodology

The experimental work includes the use of Aluminium sheets with starting dimension of 1000 × 2000 mm and with 2 mm of nominal thickness. The base material was Aluminium alloy (AA) 1050, which is the commercially available purest alloy with min. 99.5 wt% of Aluminium content according to the standard EN 573-3:2019, although the measured value was 99.7 wt% ±0.545% which was recorded by an Octane Plus energy-dispersive X-ray spectroscopy (EDX)-detector. 70 × 200 mm samples were cut for further steps by a water jet machine, preventing unnecessary heat transfer into the material. In order to facilitate the cold rolling process with the laboratory rolling mill, and to eliminate the traces of the industrial thermomechanical processes, the material was subjected to annealing at 250 °C for 60 minutes.

The sample was deformed by cold rolling on a laboratory rolling mill (Fig. 1). This equipment is equipped with two motors, which can independently turn the two rolls through the connecting planetary gears and Cardan shafts. The motors are receiving the energy through their own inverters, making it possible for the machine to individually control the speed in the two rolls i.e. asymmetric rolling. The roll gap (distance between the rolls) is adjustable through two worm gears.
Main data of the rolling mill:

- 2 pcs of 3-phase 7.5 kW motor; $M = 7750$ Nm,
- Each motor has equipped with individual planetary gear; $R = 141$ mm,
- Each motor is feed by an individual frequency inverter; $f = 25$ Hz $\longmapsto$ 50 Hz,
- Transmission: Cardan shafts,
- Rolls: $d = 150$ mm.

The initial thickness of the sample was 1.90 mm measured by caliper on multiple points, taking an average from the measurements. The first step was an asymmetric rolling with an asymmetricity ratio of 50:45 which is 1.1. The calculation is based on the applied frequency adjusted on the motor inverters. The sample thickness was reduced to 1.49 mm, consequently, the reduction has calculated as following [1]:

$$\varepsilon = \frac{h_i - h_f}{h_i} \cdot 100, \tag{1}$$

where, h_i stands for the initial thickness, and hf stands for the final thickness. The first step resulted in a 21.58% reduction. The rolled material was processed through one more symmetric rolling

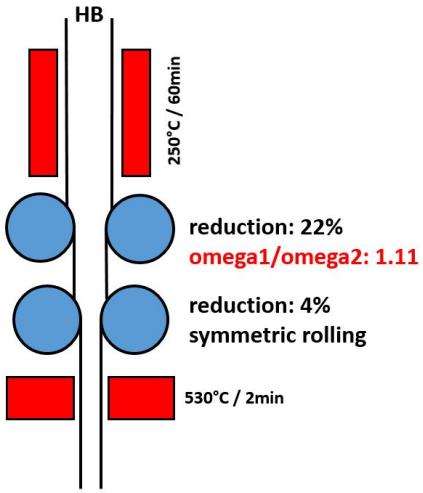

Figure 2. Flowchart of the TMP

schedules; given as the following reduction of the thickness to 1.43 mm. After cold deformation, a recrystallization annealing was performed at 530 °C for 120 s (Fig. 2).

The sample preparation for the Electron Backscatter Diffraction (EBSD) scanning includes mechanical grinding and polishing. The mechanical polishing resulted in a mirror-polished surface, which was applicable for the electrolytic polishing, which is required for the EBSD-scanning. During this process we followed the ordinary method of metallographic sample preparation, i.e. the grinding was made using wet sandpapers with grit size 400 $\longmapsto$ 600 $\longmapsto$ 800 $\longmapsto$ 1000 $\longmapsto$ 2000, and 240 rpm. The grinded sample was hand polished using Struers® polishing discs with 3 µm and 1 µm-size diamond suspensions at 400 rpm. The sample preparation was conducted in such a way that, after every step, the sample surface was cleaned by running water, cotton ball, dishwasher detergent, and dried. The electrolytic polishing for the sample was performed at 28 V for 45 s using A2 Struers electrolyte in the temperature range of 5 °C to 10 °C. The transverse direction plane (TD-plane) of the rolled sample was investigated. The prepared surface was examined by a FEI Teneo scanning electron microscope, which was equipped with the EBSD-detector. The recorded data was post-processed by the OIM-TSL-8 software. Furthermore hardness test has performed on the samples by a ZwickRoell ZHVµ hardness tester, using the Vickers-method with 500 gram-force (gf) load.

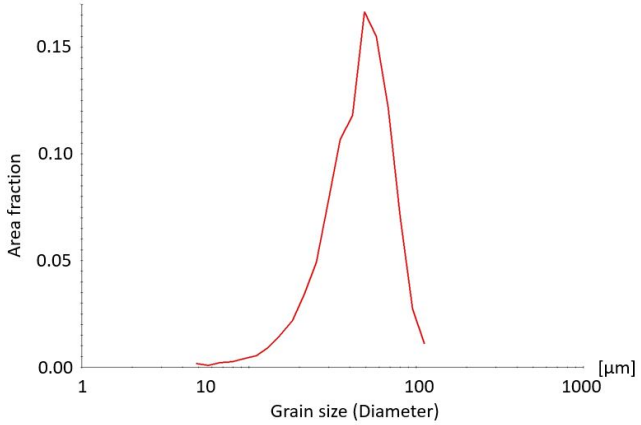

Figure 3. Grain size (diameter) in the function of area fraction

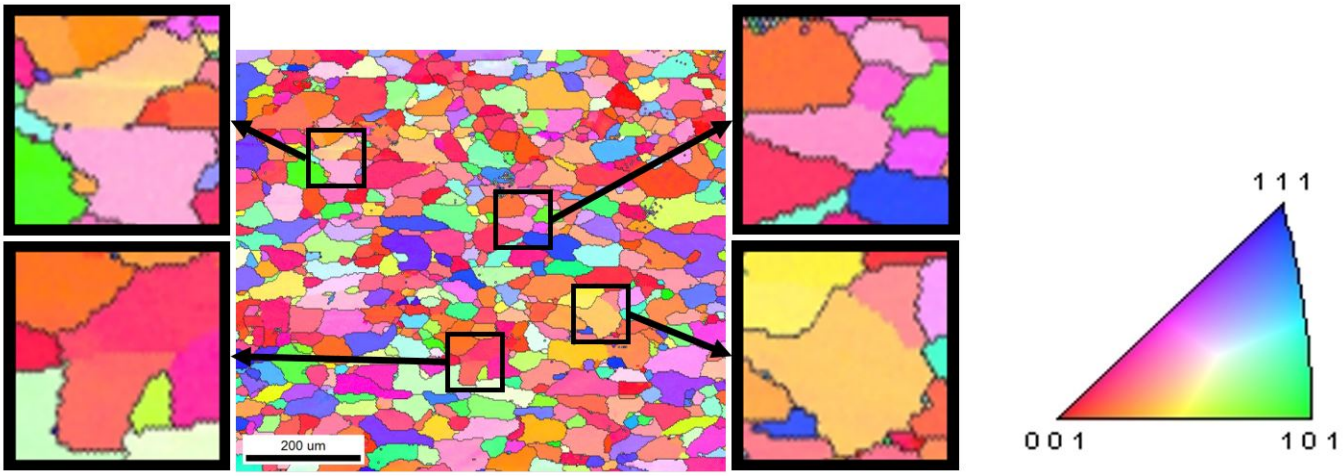

Figure 4. Microstructure of cold rolled and annealed material

3. Results

The microstructure analysis of recrystallized material reveals several grains with 0 0 1<uvw> orientation. The majority of grains have quite uniform orientation distribution, but in some cases, the low angle grain boundaries are also visible – see (Fig. 4). The average grain size of 48.5 μm was calculated by the weighted area of the grains from the distribution, shown in (Fig. 3).

In the ODF (Fig. 5), a strong Cube texture is observable with a strength up to 10.5 m.r.d (multiples of a random distribution). Apart from this, there are remaining traces of deformation texture components with relatively low intensitiy (∼1 – 1.3 m.r.d). The absence of E and F textures indicates that the shear strain was neglegibely small in the measured sample.

To better understand the TMP of the investigated material, it is important to determine the dislocation density and the stored energy (ED) after every rolling step. The stored energy is the energy originated from the formation of the dislocations and is also mentioned as the driving force for recrystallization. Since the dislocations have a direct impact on the hardness of a material, the driving force can be calculated by the following formula [27, 28]:

$$ED = \frac{H_V^2}{G \cdot (3.06M\alpha)^2}, \tag{2}$$

where the H_V is the Vickers hardness of the material in MPa (the given results are shown in (Fig. 6)),

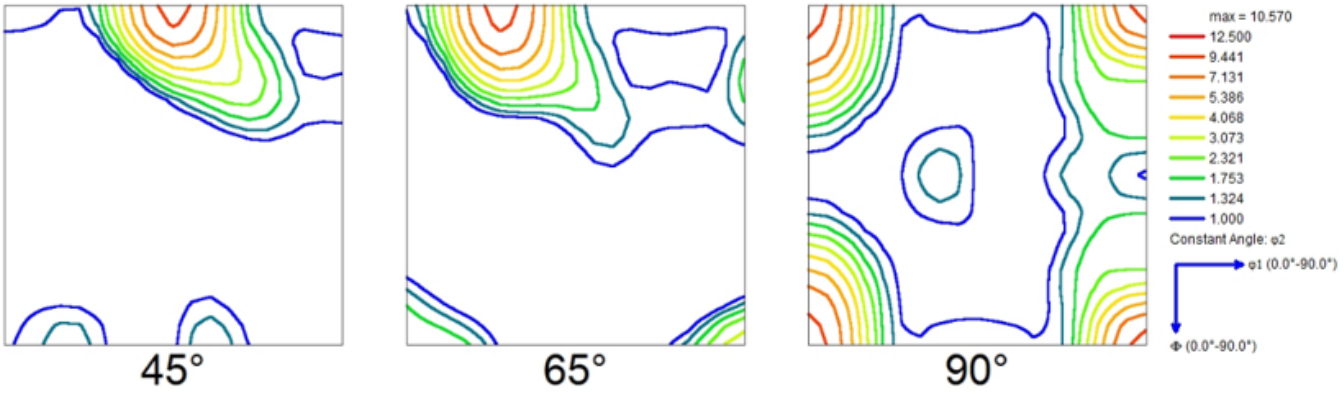

Figure 5. Texture of cold rolled and annealed material

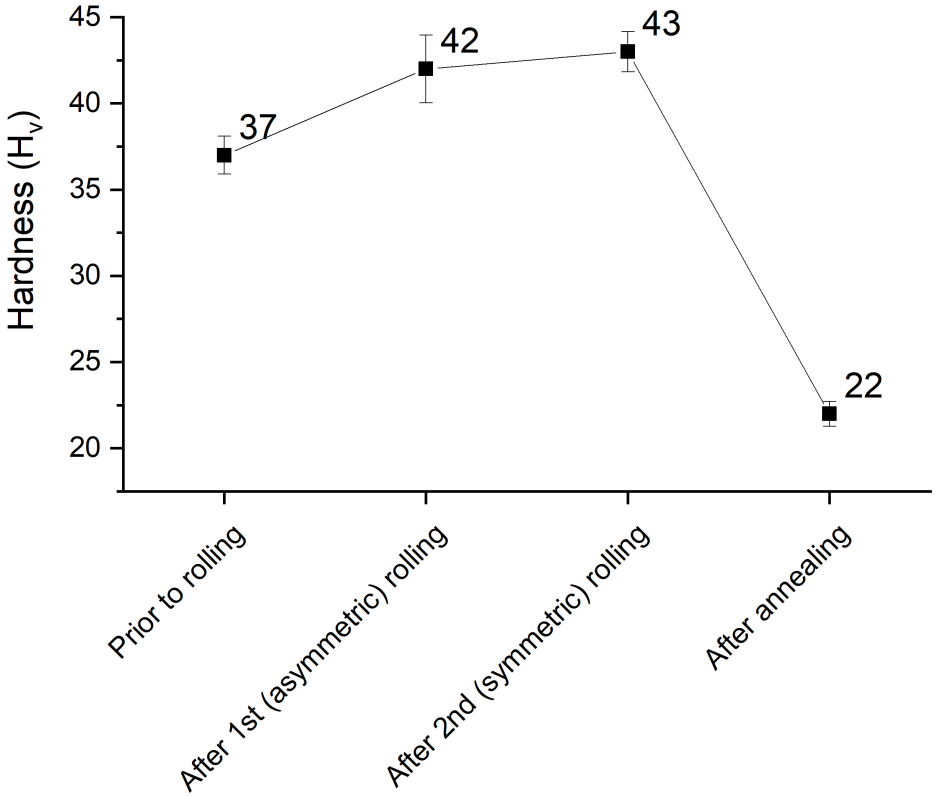

Figure 6. Change of hardness during the TMP

G is the shear modulus of Al, M is the Taylor factor, and the α is the geometric constant [13, 26, 29], it can be estimated by (3) [18]:

$$\alpha \approx \frac{1 - 0.5\nu}{4\pi(1-\nu)} \ln\left(\frac{\rho^{-0.5}}{b}\right), \tag{3}$$

where ν is 0.33 (this is typical value for high purity Al alloys) [7, 30, 31] , and ρ is the dislocation density, which was estimated by [14]. Another method for calculation stored energy is apply the formula from [13] modified using the Kubin-Estrin (KE) model is:

$$E_{D\_KE} = \alpha \cdot \rho_{\varepsilon(\mathrm{eq})} \cdot G \cdot b^2. \tag{4}$$

The calculated values of the stored energy and α are visible in Table 1.

In case of asymmetric rolling, the compressive and the possible shear strain and the equivalent

Table 1. Stored energy and α values during the rolling process

	Stored energy $\cdot 10^5$ [J/m^3]	Stored energy (Kubin-Estrin) $\cdot 10^5$ [J/m^3]	α
Sample before rolling	2.26	-	0.535
After 1st (asymmetric) rolling	2.59	3.19	0.529
After 2nd (asymmetric) rolling	2.73	3.23	0.528

strain are needed to be calculated:

$$\varepsilon_{\text{eq}} = \frac{2}{\sqrt{3}} \Phi \ln \frac{1}{\alpha_x}, \tag{5}$$

where

$$\alpha_x = \frac{h_f}{h_i}, \tag{6}$$

$$\Phi = \sqrt{1 + \left(\frac{\alpha_x^2}{1 - \alpha_x^2} \tan \Psi \right)^2}, \tag{7}$$

$$\Psi = \arctan \left(\frac{R}{2s} \left(\frac{\omega_{\text{upper}}}{\omega_{\text{lower}}} \left(\arccos \left(\frac{R - \omega_{\text{lower}} \frac{e-s}{\omega_{\text{upper}}}}{R} \right) \right) - \arccos \left(\frac{R + s - e}{R} \right) \right) \right), \tag{8}$$

$$e = \frac{h_i}{2}, \tag{9}$$

$$s = \frac{h_f}{2}, \tag{10}$$

where, R is the radius of the rolls, ω_{upper}, and ω_{lower} are the angular velocity of the upper and lower rolls respectively, and Ψ is the shear angle. During the above calculations [17], the initial equivalent strain before the first rolling step is $\varepsilon = 1.363$. This value has calculated based on the correlation of the strain and the dislocation density:

$$\frac{d\rho_m}{d\varepsilon} = \frac{C_1}{b^2} - C_2 \rho_m - \frac{C_3}{b} \sqrt{\rho_f}, \tag{11}$$

$$\frac{d\rho_f}{d\varepsilon} = C_2 \rho_m + \frac{C_3}{b} \sqrt{\rho_f} - C_4 \rho_f, \tag{12}$$

where ρ_m is the density of the mobile dislocations, ρ_f is the density of the forest dislocations, C_1 is the factor connected to mobile dislocation multiplication, $C_2 = 1.1$ 1/m^2 is the factor of the annihilation and trapping of mobile dislocations, $C_3 = 4 \cdot 10^5$ 1/m is the factor of the immobilization of them, and C_4 is the factor of the immobilization of the dislocations by the dynamic recovery. The given values are valid at 293 K [32, 33].

Prior to cold rolling the investigated material was hot rolled, and therefore large number of dislocations was generated. Although the material was annealed prior to cold rolling, the low-temperature annealing led to partial recovery, meaning that the investigated material still contains a large amount of dislocations based on the hardness test results, as it is visible in Table 2.

The sum of the forest and mobile dislocations is equals the total dislocation's amount [34]. The calculation of dislocation density, based on the hardness test, can be expressed as:

$$\rho = \frac{1}{\alpha^3} \left(\frac{H_V}{3.06 M G b} \right)^2. \tag{13}$$

Table 2. Dislocation density calculated by the indentation technique and the modified Kubin-Estrin model

	ρ $\cdot 10^{14}$ [1/m^2]	$\rho_{\varepsilon(\text{eq})}$ (Kubin-Estrin) $\cdot 10^{14}$ [1/m^2]	ε_{eq} [-]
Sample before rolling	2.106	-	1.363
After 1$^{\text{st}}$ (asymmetric) rolling	2.288	2.810	1.644
After 2$^{\text{nd}}$ (asymmetric) rolling	2.300	2.944	1.691

Another approach to determine the dislocation density is the modified Kubin-Estrin model:

$$\rho(\varepsilon_{\mathrm{eq}}) = \frac{2C_1}{C_4} - \left(\frac{2C_1}{C_4} - \rho_0\right)\left(1 + \frac{C_4\varepsilon_{\mathrm{eq}}}{2}\right)\exp\left(-C_4\varepsilon_{\mathrm{eq}}\right), \tag{14}$$

where $\rho_0 = 10^{10}$ 1/m^2 [26] is the initial dislocation density, $C_1 = 2.33 \cdot 10^{14}$ 1/m^2, and C_4 has the value of 1.2 1/m. The given parameter values are valid for 293 K [32]. The results of equivalent strain and different dislocation density calculations are presented in Table 2.

During the calculations of the dislocation density and stored energy, the equivalent strain of the sample before the first rolling step ad the indentation-based dislocation density were determined with the $\alpha = 0.5$, since in the case of high strains the α tends to saturate to this value [26]. For each strain increment the equivalent strains were added to each other, as displayed in Table 2.

4. Discussion

The reported data suggests that, after the initial rolling, the orthorhombic symmetry remained intact due to the lower level of asymmetricity mainlined during the rolling experiments. The presence of Cube texture is typically observed after conventional rolling and the following recrystallization. The integrity of the orthorhombic ODF symmetry and the lack of E and F shear textures can be originated from the low-level i.e. 50/45 asymmetricity; although this level was sufficient for the appearance of a weak H shear texture. The overall symmetric-like rolling is the reason for the ordinary Cube- and β-fiber – type textures.

The minimal rise in the hardening after the second rolling pass can be originated from the low level additional deformation i.e. after a 22% reduction by an asymmetric rolling pass, a symmetric 4% reduction was performed which exposes the sample to a minimal normal strain.

The current study clearly depicts the fact that a 50/45 asymmetricity level is not sufficient in the case of 1050 aluminium alloy to reach a substantial level of shear texture, thus a significantly higher level of asymmetry is needed to reach the desired H, E, and F texture, and to destroy the Cube texture at the same time. The dislocation densities as well as the stored energies, predicted by the indentation technique and K-E model are of the same order of magnitude. The deviations between the measured and calculated values can be explained by the simplifications, made in the modified K-E approach.

5. Conclusion

Results of the current investigation show that the low level of asymmetry is not capable of modifying the conventional texture, which tends to appear during thermomechanical processing. The higher degree of asymmetricity might provide a desirable shear-type texture. The estimated dislocation density and driving force for recrystallization are correlated well with the data presented in various literature sources. The deviations observed between the measured and calculated counterparts might emerge from the simplifications made in the modeling approaches.

6. Acknowledgement

Project no. TKP2021-NVA-29 has been implemented with the support provided by the Ministry of Innovation and Technology of Hungary from the National Research, Development and Innovation Fund, financed under the TKP2021-NVA funding scheme.

7. References

[1] ME Mechanical Team, *Defects in Sheet Metal Drawing*, CrossRef

[2] O.M. Ikumapayi, S.A. Afolalu, J.F. Kayode, R.A. Kazeem, S. Akande, *A concise overview of deep drawing in the metal forming operation*, Materials Today: Proceedings 62, 2022, pp. 3233–3238, CrossRef

[3] J. Sidor, R.H. Petrov, L.A.I. Kestens, *Deformation, recrystallization and plastic anisotropy of asymmetrically rolled aluminum sheets*, Materials Science and Engineering: A 528(1), 2010, pp. 413–424, CrossRef

[4] J. Herrmann, M. Merklein, *Improvement of deep drawability of ultra-fine grained 6000 series aluminum alloy by tailored heat treatment*, Procedia Manufacturing 15, 2018, pp. 976–983, CrossRef

[5] J.G. Lenard, M. Pietrzyk, L. Cser, *Mathematical and physical simulation of the properties of hot rolled products*, Amsterdam Lausanne New York: Elsevier, 1999.

[6] O. Engler, K. Knarbakk, *Temper rolling to control texture and earing in aluminium alloy AA 5050A*, Journal of Materials Processing Technology 288, 2021, p. 116910, CrossRef

[7] W.D. Callister, *Materials science and engineering: an introduction*, 7th ed. New York: John Wiley & Sons, 2007.

[8] X. Bian, L. Heller, L. Kadeřávek, P. Šittner, *In-situ synchrotron X-ray diffraction texture analysis of tensile deformation of nanocrystalline NiTi wire in martensite state*, Applied Materials Today 26, 2022, p. 101378, CrossRef

[9] W.Q. Gao, C.L. Zhang, M.X. Yang, S.Q. Zhang, D. Juul Jensen, A. Godfrey, *Strain distribution and lattice rotations during in-situ tension of aluminum with a transmodal grain structure*, Materials Science and Engineering: A 828, 2021, p. 142010, CrossRef

[10] S. Nishikawa, S. Kikuchi, *Diffraction of Cathode Rays by Mica'*, Nature 121(3061), 1928, pp. 1019–1020, CrossRef

[11] O. Engler, V. Randle, *Introduction to texture analysis: macrotexture, microtexture, and orientation mapping*, 2nd ed. Boca Raton: CRC Press, 2010.

[12] S.I. Wright, R. Hielscher, *Structures: Orientation texture*, in Reference Module in Materials Science and Materials Engineering, Elsevier, 2022, p. B9780323908009000000, CrossRef

[13] F.J. Humphreys, M. Hatherly, *Recrystallization and Related Annealing Phenomena*, Elsevier, 1995, CrossRef

[14] S.H. Kim, J.H. Ryu, K.H. Kim, D.N. Lee, *The Evolution of Shear Deformation Texture and Grain Refinement in Asymmetrically Rolled Aluminum Sheets*, Journal of the Society of Materials Science 51(3), 2002, pp. 20–25, CrossRef

[15] D.N. Lee, H.J. Shin, S.H. Hong, *The Evolution of the Cube, Rotated Cube and Goss Recrystallization Textures in Rolled Copper and Cu-Mn Alloys*, KEM 233–236, 2003, pp. 515–520, CrossRef

[16] H. Jin, D.J. Lloyd, *The different effects of asymmetric rolling and surface friction on formation of shear texture in aluminium alloy AA5754*, Materials Science and Technology 26(6), 2010, pp. 754–760, CrossRef

[17] J. Sidor, R.H. Petrov, L. Kestens, *Texture Control in Aluminum Sheets by Conventional and Asymmetric Rolling*, Comprehensive Materials Processing 3, 2014, pp. 447–498, CrossRef

[18] W. Truszkowski, J. Kr'ol, B. Major, *Inhomogeneity of rolling texture in fcc metals*, MTA 11(5), 1980, pp. 749–758, CrossRef

[19] W. Truszkowski, J. Krol, B. Major, *On Penetration of Shear Texture into the Rolled Aluminum and Copper*, MTA 13(4), 1982, pp. 665–669, CrossRef

[20] M.Y. Amegadzie, D.P. Bishop, *Effect of asymmetric rolling on the microstructure and mechanical properties of wrought 6061 aluminum*, Materials Today Communications 25, 2020, p. 101283, CrossRef

[21] O.V. Mishin, B. Bay, G. Winther, D.J. Jensen, *The effect of roll gap geometry on microstructure in cold-rolled aluminum*, Acta Materialia 52(20), 2004, pp. 5761–5770, CrossRef

[22] H. Jin, D.J. Lloyd, *The reduction of planar anisotropy by texture modification through asymmetric rolling and annealing in AA5754*, Materials Science and Engineering: A 399(1–2), 2005, pp. 358–367, CrossRef

[23] B. Beausir, S. Biswas, D.I. Kim, L.S. Tóth, S. Suwas, *Analysis of microstructure and texture evolution in pure magnesium during symmetric and asymmetric rolling*, Acta Materialia 57(17), 2009, pp. 5061–5077, CrossRef

[24] S. Wronski, B. Ghilianu, T. Chauveau, B. Bacroix, *Analysis of textures heterogeneity in cold and warm asymmetrically rolled aluminium*, Materials Characterization 62(1), 2011, pp. 22–34, CrossRef

[25] Horváth László, *Mélyhúzás lemezanyagai és minősítési módszereik*, Óbudai Egyetem, Bánki Donát Gépész és Biztonságtechnikai Mérnöki Kar, Anyagtudományi-és Gyártástechnológiai Intézet, 2009.

[26] J.J. Sidor, P. Chakravarty, J.Gy. Bátorfi, P. Nagy, Q. Xie, J. Gubicza, *Assessment of Dislocation Density by Various Techniques in Cold Rolled 1050 Aluminum Alloy*, Metals 11(10), 2021, p. 1571, CrossRef

[27] M. Taheri, H. Weiland, A. Rollett, *A method of measuring stored energy macroscopically using statistically stored dislocations in commercial purity aluminum*, Metallurgical and Materials Transactions A 37(1), 2006, pp. 19–25, CrossRef

[28] A.A. Saleh, P. Mannan, C.N. Tomé, E.V. Pereloma, *On the evolution and modelling of Cube texture during dynamic recrystallisation of Ni–30Fe–Nb–C model alloy*, Journal of Alloys and Compounds 748, 2018, pp. 620–636, CrossRef

[29] G.E. Dieter, *Mechanical metallurgy 3. ed*, London Hamburg: McGraw-Hill, 1988.

[30] J.J. Sidor, K. Decroos, R.H. Petrov, L.A.I. Kestens, *Evolution of recrystallization textures in particle containing Al alloys after various rolling reductions: Experimental study and modeling*, International Journal of Plasticity 66, 2015, pp. 119–137, CrossRef

[31] J.J. Sidor, *Assessment of Flow-Line Model in Rolling Texture Simulations*, Metals 9, 2019, p. 21, CrossRef

[32] T. Csanádi, N.Q. Chinh, J. Gubicza, G. Vörös, T.G. Langdon, *Characterization of stress–strain relationships in Al over a wide range of testing temperatures*, International Journal of Plasticity 54, 2014, pp. 178–192, CrossRef

[33] L.P. Kubin, Y. Estrin, *Evolution of dislocation densities and the critical conditions for the Portevin-Le Châtelier effect*, Acta Metallurgica et Materialia 38(5), 1990, pp. 697–708, CrossRef

[34] T. Csanádi, N.Q. Chinh, J. Gubicza, T.G. Langdon, *Plastic behavior of fcc metals over a wide range of strain: Macroscopic and microscopic descriptions and their relationship*, Acta Materialia 59(6), 2011, pp. 2385–2391, CrossRef